1-1-2016

Creation Of Novel Inducible Cell Line To Study Alveolar Rhabdomyosarcoma

Kaoru Takasaki
Yale University

Creation of novel inducible cell line to study alveolar rhabdomyosarcoma

A Thesis Submitted to the
Yale University School of Medicine
in Partial Fulfillment of the Requirements for the
Degree of Doctor of Medicine

by

Kaoru Takasaki

2016

ABSTRACT

CREATION OF NOVEL INDUCIBLE CELL LINE TO STUDY ALVEOLAR RHABDOMYOSARCOMA. Kaoru Takasaki, Ranjini K. Sundaram, Ranjit S. Bindra. Departments of Therapeutic Radiology and of Pathology, Yale University, School of Medicine, New Haven, CT.

Rhabdomyosarcoma (RMS) is a group of relatively rare mesenchymal malignancies classically associated with skeletal muscle and most frequently seen in the pediatric population. While chemotherapy, radiation, and surgical resection can confer long-term event-free survival rates of up to 85-95%, the prognosis for alveolar rhabdomyosarcoma (ARMS), particularly those positive for either the t(2;13) PAX3-FOXO1 or t(1;13) PAX7-FOXO1 translocation, is significantly worse. As such, the development of therapies that are specific for fusion-positive ARMS cells are of particular clinical interest, and it has been suggested that the concept of synthetic lethality can be exploited to target genes that become essential for cellular survival only in the presence of PAX3/7-FOXO1 expression. A stable tetracycline-inducible PAX3-FOXO1 clonal cell line in a U2OS background is created here in order to study in isolation the effects of the fusion protein on tumor response to novel chemotherapeutic agents. The cell line's validity as a genetic mimic of PAX3-FOXO1 positive ARMS is verified by testing via qPCR the upregulation of DAPK, FGFR4, GREM1, and MyoD, which serve as proxies for global gene expression changes in fusion-positive ARMS, in the induced vs. uninduced states. DAPK and MyoD consistently demonstrate a statistically significant upregulation, as expected, but data for FGFR4 and GREM1 are inconclusive. Although additional experiments therefore need to be conducted to fully

confirm that the inducible cell line indeed exhibits the transcriptional reprogramming seen in PAX3/7-FOXO1 positive ARMS, the data so far support this hypothesis. Ultimately, this cell line will be used in a high-throughput assay to identify chemotherapeutic agents that preferentially kill those with PAX3-FOXO1 expression, with the hopes of improving the poor prognosis that fusion-positive ARMS patients currently face.

ACKNOWLEDGEMENTS

I would first like to express my sincere gratitude to my PI and thesis advisor, Professor Ranjit Bindra, for providing constant motivation, insight, and support for my research. His understanding of the demands of medical school was pivotal in ensuring the progress of my research. I must also thank Ranjini Sundaram, Ph.D., who often maintained cell cultures and carried out parts of my project in my absence, and the other members of the Bindra Lab who offered advice and encouragement throughout. The Barr Lab (National Cancer Institute), Jensen Lab (Yale School of Medicine), and Glazer Lab (Yale School of Medicine) generously provided materials and expertise that greatly assisted my research.

I am also immensely grateful to Professor Benjamin Gewurz (Harvard Medical School) for introducing me to the joys and rigors of strong scientific research, and for patiently teaching me all of my foundational bench skills.

This research was supported by the Alex's Lemonade Stand Foundation Pediatric Oncology Student Training (POST) Program Grant (2013), the Yale First Year Summer Student Fellowship (2013), and the Cure Search Young Investigator-2 Grant (awarded to Professor Bindra, 2015-2018).

TABLE OF CONTENTS

I. INTRODUCTION

Rhabdomyosarcoma (RMS) is a group of mesenchymal malignancies classically associated with skeletal muscle but also frequently found in other parts of the body such as the head, neck, biliary tract, and urogenital tract. While they are the most common soft-tissue tumors and the third most common extracranial solid tumors in the pediatric population, they are still relatively rare overall, with incidence rates of 0.5-0.6 per 100,000 in patients 0-14 years of age (1) and an estimated 350 new cases in the United States each year (2). Among the various subtypes of RMS, alveolar rhabdomyosarcoma (ARMS) is distinct in its epidemiology, prognosis, and genetic signature. It is typically found in older children and teenagers, although two-thirds of RMS patients overall are diagnosed before their sixth birthday (3), and patients more often present with metastatic disease at the time of diagnosis compared to other subtypes (4). The latter tendency is at least in part explained by the fact that RMS begins as an asymptomatic mass, with or without accompanying mass effects, and such masses in adolescents are often attributed to a musculoskeletal injury (3). This delay in presentation and diagnosis carries unfavorable implications for prognosis; ARMS patients are automatically stratified into at least the intermediate risk category, and while treatment with chemotherapy, radiation, and/or surgery currently allows 60-70% of ARMS patients with localized disease to survive long-term, the long-term event-free survival rate for those with metastatic disease is as low as 15%. In contrast, patients with the more favorable embryonal rhabdomyosarcoma (ERMS) see long-term event-free survival rates of up to 85-95% if localized or completely resected, and approximately 35% if metastatic (5). Early diagnosis and effective treatment of ARMS therefore remains a clinical challenge.

ARMS cases can be further be subclassified into fusion-positive and fusion-negative;

50-80% of ARMS tumors carry either the more common t(2;13) PAX3-FOXO1 (PAX3-FKHR) or the less common t(1;13) PAX7-FOXO1 (PAX7-FKHR) chromosomal translocation (2, 3, 6-10), while the rest are alveolar in histology but lack a characteristic genetic signature. These translocations also carry prognostic implications, and PAX3-FOXO1 in particular has been associated with unfavorable outcomes. In one study, the estimated 5-year survival rates for PAX3-FOXO1, PAX7-FOXO1, and fusion-negative ARMS were 39%, 74%, and 89%, respectively (11). Another study found that 4-year survival overall for PAX3-FOXO1 patients was 52% as opposed to 77% for PAX7-FOXO1 patients; even more impressively, the respective 4-year survival rates for those with metastatic disease were 8% and 75% (10). Within a clinical trial comparing two chemotherapy protocols, 5-year event-free survival and overall survival rates for fusion-negative ARMS ranged between 80-100%, versus 49-92% for fusion-positive ARMS (9). In light of these data, the functions of PAX3/7-FOXO1 fusion proteins and their potential as targets for directed therapy have been the focus of much investigation.

PAX3 and PAX7 are both transcription factors that are critical in tissue development; PAX3 regulates neural crest development and embryonic skeletal muscle formation, and has anti-apoptotic effects, while PAX7 plays a larger role in post-natal myogenesis and adult muscle regeneration (12). FOXO1 is an insulin-regulated forkhead transcription factor that is involved in the control of glucose metabolism, cell cycle progression, and apoptosis (13). When fused, PAX3/7-FOXO1 acts upstream via multiple molecular pathways to powerfully stimulate cellular proliferation, angiogenesis, cellular transformation, and myogenesis, and inhibit apoptosis and terminal differentiation (7, 14); one such mechanism that has been proposed for PAX7-FOXO1 is prevention of the downregulation of NF-kB that normally

occurs with terminal differentiation of muscle cells (14). The wide-ranging consequences of acting upstream are magnified by the fact that not only are the fusion proteins expressed at higher levels than wildtype PAX3/7, but also that they are 10- to 100-fold more potent transcription factors than wildtype PAX3/7 (15). Additionally, unlike wildtype FOXO1, PAX3/7-FOXO1 does not translocate from the nucleus to the cytoplasm for proteasomal degradation and instead remains constitutively active (15, 16).

Interestingly, comparisons of ARMS to ERMS as well as of fusion-positive ARMS to ERMS and fusion-negative ARMS reveal distinct patterns of genetic alterations. In general, gains of either partial or whole chromosomes, particularly of chromosomes 2, 5, 7, 8, 11, 12, 13, 17, 18, and 19, and less frequently losses of chromosomes 10, 14, 15, 16, and 19, have been more closely associated with ERMS than with ARMS (17-19); a review of comparative genomic hybridization analyses concluded that chromosome-level changes—apart from the obvious t(2;13) and t(1;13) translocations—are indeed less commonly seen in ARMS tumors (8). These studies have found that instead, ARMS cells exhibit copy-number variations more commonly than ERMS cells (8, 17-19). Among the amplified genes are CDK4, an oncogene implicated in a number of malignancies including glioblastoma, liposarcoma, melanoma, and breast carcinoma; MYCN, a transcription factor associated with neuroblastoma and retinoblastoma; and MIR17HG, the host gene for a microRNA cluster that is also amplified in diffuse large B-cell lymphoma and small cell lung carcinoma (8, 18, 20). Also amplified are genes involved in signaling pathways, such as cell surface receptors WNT1 and PDGFB (20); tyrosine kinase receptors ErbB2 (20) (amplified in breast and ovarian carcinomas), ErbB3 (20) (amplified in prostate, bladder, and breast carcinomas), and ALK (21, 22) (amplified in anaplastic large cell lymphomas, neuroblastoma, and non-small cell lung

cancer); MAPK cascade player RAF1 (20); and tyrosine kinase PTK2 (20). Some amplified stretches have also been associated with poorer clinical outcomes for both fusion-positive and -negative ARMS: IRS2 has anti-apoptotic functions and has been associated with increased metastatic potential in breast cancer (21), while 2q13-q14 does not correspond with a known gene (18).

Furthermore, PAX3/7-FOXO1 positive tumor cells have been shown to carry fewer gene mutations than their fusion-negative counterparts, and it has been suggested that both this and the limited number of chromosomal changes reflect the critical role of "transcriptional reprogramming" in the pathophysiology of fusion-positive ARMS (18). The relatively few mutations that are seen in fusion-positive tumors are usually common to both subsets of ARMS as well as ERMS; these include genes involved in cell cycle regulation, protein phosphorylation, DNA repair, muscle cell differentiation, MAPK regulation, chromatin modification, and induction of apoptosis. Among these are PIK3CA, which functions in cell proliferation and has been implicated in cervical, papillary thyroid, squamous cell, and breast carcinomas; BCOR, a transcription repressor that may play a role in apoptosis; ATM, which regulates the rate of cell division and is also involved in DNA repair; and ZNF350, which is a transcriptional repressor that has been associated with neuromas (18). Notably, mutations in RAS are among the most common seen fusion-negative RMS, but have not been found in fusion-positive cells (18, 21).

In light of the relative dearth of mutations in genes classically associated with malignancy, the true genetic hallmarks of fusion-positive ARMS lie in patterns of gene expression—the "transcriptional reprogramming" reflective of PAX3/7 and FOXO1's native functions as transcription factors—as evidenced through cDNA microarrays, RNA profiles,

and DNA methylation profiles. Although multiple genes have been found to be universally upregulated or downregulated in ERMS, fusion-negative ARMS, and fusion-positive ARMS, a number of affected genes have been specifically associated with PAX3-FOXO1, PAX7-FOXO1, or both. Many more upregulated than downregulated genes have been reported in the literature (6, 14, 23-31). Induced transcriptional targets of functional interest include MyoD (6, 23, 25), myogenin (25), IGFBP5 (25), PTMA (32), FGFR4 (6, 14, 29, 31), homeobox genes (27, 29), PTHLH (24), NELL1 (6, 29), ELMO1 (29), CPT1A (27), SLIT2 (24), SLUG (25), and MYCN (6, 28); although the mechanisms by which their protein products contribute to ARMS' malignant properties have not been fully elucidated, taken together they appear to dually repress myogenic differentiation and promote cell survival (6). A complete list of differentially expressed genes as reported in the literature as of 2013 can be found in Supplementary Table 1.

Unsurprisingly, a number of these upregulated proteins play roles in myogenesis. Myogenin and MyoD are both transcription factors that apparently induce the expression of other genes that regulate muscle growth, energy metabolism, and contractility; of these, MYL4 is particularly intriguing because it is a fetal muscle gene that is not found in adult myocytes (25). Myogenin is also known to induce the expression of IGFBP5 in both normal and PAX3-FOXO1 cells; the protein is secreted during embryonic muscle development, and binds to IGF1 and IGF2 to modulate their effects on growth. PTMA, which among its multiple studied functions also has a strong link with cellular growth and survival, has been associated with myogenic proliferation. Meanwhile FGFR4, normally under the control of PAX3 and PAX7, is expressed in the very early stages of muscle differentiation. The upregulation of these genes is in line with the repression of PMX1 (25), which is typically

expressed in adult skeletal muscle, and overall with PAX3/7-FOXO1's ability to inhibit terminal muscle tissue differentiation.

Also playing a key role in tissue differentiation and overall embryonic development are the homeobox genes, SLUG, and MYCN. Upregulated in PAX3-FOXO1 cells are HOXA9 (27, 29), which regulates embryonic gene expression, morphogenesis, and tissue differentiation; HOXB13 (27), which is involved in fetal skin development and later, cutaneous regeneration; and HOXD1 (27), which functions in tissue differentiation and limb development. SLUG is a zinc finger transcriptional repressor that is related to neural crest and limb bud development as well as epithelial-mesenchymal transitions; importantly, its protein has anti-apoptotic activity and is also thought to repress E-cadherin transcription in breast carcinoma. MYCN, also found to be amplified in analyses of copy-number variation, is expressed in the normal embryo to play critical roles in neurological development.

Associated with enhanced tumor cell migration are PTHLH, NELL1, ELMO1, and CPT1A. ELMO1 endogenously promotes cytoskeletal rearrangements and phagocytosis, but the native roles for the other proteins are less intuitive. PTHLH, broadly involved in endochondral bone development, has been implicated in the metastases of breast carcinomas and RMS to the bone. NELL1 also plays a role in bone growth and activates components of the MAPK cascade. Finally, CPT1A, classically understood as a regulatory enzyme in fatty-acid oxidation, has more recently been studied in the context of apoptosis and cell proliferation as well as metastatic potential. Assisting this propensity for increased metastasis is SLIT2, which not only has a role in axonal guidance but also recruits endothelial cells to promote angiogenesis.

Despite these wide-ranging transcriptional changes, it has been demonstrated via both

mouse models and human tissue that PAX3/7-FOXO1 by itself is generally insufficient for tumorigenesis (7, 18, 25), and in fact isolated overexpression can result in cellular growth suppression or even death (16, 33). Although the introduction of a fusion gene causes accelerated growth and occasionally malignant transformations *in vitro*, preliminary research in mice has demonstrated that the expression of PAX3-FOXO1 causes developmental abnormalities such as cardiac and diaphragmatic defects (34), but no muscle tumors (34, 35). However, tumors are observed *in vivo* or on soft agar when the fusion proteins are combined with inactivation of p53 or constitutive Ras pathway activation (35). In human skeletal muscle cells, PAX3-FOXO1 expression and $p16^{INK4A}$ methylation, the latter which in turn disables the Rb pathway, act synergistically to allow these cells to more quickly bypass the "senescence checkpoint" than either of these genetic events alone (33). This checkpoint typically marks the beginning of a period resulting in terminal differentiation and growth arrest, though it appears that PAX3-FOXO1 and $p16^{INK4A}$ affects growth only (33). Further research has shown that $p14^{ARF}$, another tumor suppressor, is also downregulated in PAX3-FOXO1 positive cells; additionally, upregulation of hTERT, involved in telomere stabilization, and MYCN are required for tumorigenesis in cells expressing PAX3-FOXO1 with $p16^{INK4A}$ and $p14^{ARF}$ loss of function (36).

Other genes upregulated in fusion-positive ARMS cells also appear to depend on the particular genetic milieu of the tumor. For instance, NELL1 overexpression has been shown to induce apoptosis in normal myoblasts yet contributes to increased invasiveness in fusion-positive cells, leading to the suggestion that the advantageous effects of NELL1 may be dependent on the fusion or additional proteins present only in the tumor (29). This further emphasizes that PAX3/7-FOXO1 positivity does not act alone or independently in

establishing ARMS' oncological properties.

That PAX3/7-FOXO1 cells require additional genes to complete their malignant transformation and subsequently survive suggests that these ARMS cells are dependent on these and other genes for survival. Indeed, all cancers are characterized by a paradoxical relationship to DNA repair mechanisms: although they must hijack DNA repair pathways in order to undergo tumorigenesis, they simultaneously require intact DNA repair pathways in order to continue to replicate their genetic material and divide; in other words, the tumor becomes dependent on an intact alternative DNA repair mechanism or cellular survival gene (37-39). Survival genes encompass all of those that enable cancerous cells to evade immune surveillance and withstand the additional metabolic, proteotoxic, mitotic, oxidative, and DNA damage stresses brought on by uncontrolled proliferation and survival (40). This model of dependency, known as oncogene addiction, has been studied extensively in breast and ovarian cancers arising from BRCA1 or BRCA2 mutations (38, 41-43). In the case of these malignancies, PARP1, a critical player in the repair of single-strand breaks, becomes essential as BRCA1 and BRCA2 can no longer regulate the repair of double-stranded breaks; without PARP1, double-stranded DNA breaks accumulate, thereby stalling DNA replication and cell growth (38, 43). PARP1 inhibition has therefore gathered much attention as a potential therapy, and takes advantage of the related, emerging concept of synthetic lethality.

Synthetic lethality, originally defined over a century ago in *Drosophila melanogaster* but not applied to cancer research until fairly recently, refers to a relationship between two genes in which a mutation in one will not impact a cell's viability, whereas mutations in both will result in cell death. The traditional conceptualization centers on two genes that function in redundant pathways or converge on a common critical pathway, typically in DNA repair

but also in other processes, in such a way that one can compensate for the loss of the other (37-39, 41-43). This redundancy is understood to contribute to genetic robustness, which allows organisms to maintain homeostasis and survive in the face of varied environmental perturbations and evolutionary challenges (42). An offshoot of synthetic lethality, known as "synthetic dosage lethality," refers to a relationship in which one upregulated gene requires the upregulation of another for the cell to survive (38). Because by definition, healthy cells should not harbor deactivating or activating mutations in or abnormal levels of expression of any of these genes, targeting a synthetically lethal gene should affect only the tumor. The effects can be categorized into two groups: "stress sensitization," which hampers the cells' ability to endure the aforementioned five categories of additional stresses, and "stress overload," which increases the burden posed by these stresses (40). Both strategies tackle the significant challenges to effective targeted cancer therapies, the need for which is highlighted by the fact that the majority of available cancer treatments are extremely toxic to patients.

Currently used chemotherapeutic agents typically have low therapeutic indices and narrow therapeutic windows, rendering the appropriate dosing of these drugs very difficult (44). Although most chemotherapies attempt to exploit the fact that cancer cells are growing and dividing more quickly than their healthy counterparts, they nonetheless target enzymes that are common to both types of cells and cause well-known side effects such as hair loss and gastrointestinal upset. Furthermore, the inherent lack of specificity in most existing chemotherapies opens the door to the development of resistance for which the mechanisms are unclear; in contrast, knowing the genetic targets enables treatment protocols to anticipate or even prevent resistance (41). While success stories such as imatinib against BCR-ABL in chronic myelogenous leukemia exist, in general the search for targeted treatments has been

elusive. Oncogenes are often more similar to their non-mutated counterparts than not, and tumor suppressors with loss of function generally cannot be adequately restored via pharmacological means (37, 40, 41, 44, 45). Harnessing synthetic lethality allows medicine to sidestep the most obvious target, and it is thus particularly appealing for the treatment of malignancies characterized by the upregulation of non-kinases such as KRAS, which cannot be blocked without impairing signaling activity in normal cells (39).

Candidate genes for a synthetically lethal therapeutic target are therefore most likely upregulated in the tumors of interest, and for fusion-positive ARMS include but are not limited to those discussed above. Of the genes that comprise ARMS' genetic signature, MYCN and the MYC family, which like KRAS are difficult to target but frequently upregulated in cancer, have been the focus of much investigation albeit in non-RMS contexts. Previous research has demonstrated that the CDK family is in a synthetically lethal relationship with overexpressed MYCN. Inhibition of CDK2 in neuroblastoma cells induced an upregulation of p53 and subsequent apoptosis (46), while inhibition of CDK1 in a panel of human tumor cell lines caused apoptosis secondary to downregulation of the apoptosis inhibitor BIRC5 (47). Other studies have shown that AURKB, which regulates mitosis, is synthetically lethal to MYC and MYCN by inducing apoptosis independently of p53 expression (48, 49). siRNA silencing of GSK3β, a serine-threonine kinase that functions in the negative regulation of glucose homeostasis and Wnt signaling, causes apoptosis in MYC-overexpressing cells through downstream upregulation and potentiation of the TRAIL death receptor DR5 (50, 51).

Synthetically lethal relationships for which the molecular mechanisms are less clear have also been found. Knockdown of TDP1 and inhibition of PARP1, which are both

components of a larger single-strand DNA break repair complex, results in apoptosis in ARMS cells, suggesting that these two proteins are compensating for a hitherto unidentified defective DNA repair mechanism (52). It also enhances the ARMS response to the topoisomerase I inhibitor camptothecin (52). While the inhibition of two targets before chemotherapy is unlikely to be clinically feasible, this result exemplifies the wide range of applications of synthetic lethality, from the identification of specific targets and development small-molecule inhibitors to increasing the effectiveness of existing therapies. This finding is also particularly intriguing in light of the fact that fusion-positive ARMS has been shown to be more responsive to camptothecin therapy than ERMS via a mechanism independent of topoisomerase I inhibition; it raises the possibility that this chemotherapy acts on a downstream target of PAX3/7-FOXO1 that is synthetically lethal to the tumor (53), perhaps related to the same unidentified defective DNA repair mechanism.

While these results are encouraging, the heterogeneity of fusion-positive ARMS genetics and patient physiologies necessitates further research into additional synthetically lethal targets. RNAi screens, high-throughput chemical screens, and combined RNAi/small-molecule screens are the most common approaches to the therapeutic exploitation of synthetic lethality (54). For the purposes of using synthetically lethal relationships, RNAi screens typically employ reverse genetics, which starts with the cancer cell line under study and attempts to detect the functional consequences of inhibiting the expression of a wide range of genes (42). The results are culled for gene targets that cause such desired effects as decreased cell viability, motility, and mitotic activity when inhibited in the cell line of interest but not in others. This thus plays upon oncogene addiction and synthetic lethality but is notably limited by off-target effects and dose-specific phenotypic responses (42, 45). The

initial screen is followed by validation of the identified targets *in vivo*, and, if successful, high-throughput chemical screens to find existing or new drugs that act upon the genes' protein products.

It is also possible to bypass the initial step of identifying synthetically lethal genes, and instead begin with the high-throughput chemical screen to immediately search for existing drugs that selectively kill the cancer cells of interest without necessarily knowing the protein target. As in the likely case of camptothecin, this intrinsically exploits a synthetically lethal relationship. This approach is most limited by off-target effects as well as the fact that chemical compounds can behave differently *in vitro* and *in vivo*, and therefore be unsuitable for clinical use despite exhibiting desired inhibitory effects in the screen (45, 54). Not knowing the molecular targets of an identified drug potentially allows for more unanticipated side effects *in vivo*, and the process of working in reverse to find the molecular target can be labor-intensive. The combined RNAi/small-molecule screen attempts to address these limitations by simultaneously identifying drugs and RNAi knockdowns that achieve the same phenotype, and cross-comparing the results to find a chemical compound that inhibits the protein product (45). Although this type of screen is expensive and still comparatively nascent, knowing the intended target of a drug increases the likelihood that it will meet the criteria for clinical usability.

RNAi and high-throughput chemical screens are themselves not new research strategies. Yet applying the concept of synthetic lethality to these methods enhances the specificity of the results, and in theory increases the yield of the lead optimization process upon which all three screening tactics converge. Here, it is hoped that by taking advantage of genetic relationships that are exclusive to fusion-positive ARMS, the relative

unresponsiveness of these tumors to existing chemotherapy- and radiation-based treatments, and the consequent poor prognosis, can begin to be addressed.

II. STATEMENT OF PURPOSE

This thesis aims to create and characterize a stable, inducible PAX3-FOXO1 clonal cell line in a U2OS background to enable the eventual study of the fusion protein's downstream effects with respect to drug response. The validity of this clonal cell line as a mimic of fusion-positive ARMS will be verified by comparing its cDNA profile for four proxy genes to those previously reported in the literature and to cDNA data obtained for U2OS, fusion-negative RMS, and fusion-positive ARMS cell lines.

Fusion status is closely linked to prognosis and patient outcomes in ARMS, and a greater understanding of the unique properties PAX3/7-FOXO1 confers upon tumor cells is likely key to the development of better therapies. The PAX3-FOXO1 inducible cell line allows for the investigation of the fusion protein's effects in isolation, independent of other genetic changes that may be common to both fusion-positive and -negative ARMS. More precisely, this allows for the identification of genetic relationships that are synthetically lethal to PAX3-FOXO1 specifically.

Ultimately, these clonal cell lines will be used alongside control ARMS, ERMS, and U2OS cells in a high-throughput chemical screen to identify drug compounds that selectively kill PAX3-FOXO1 expressing cells. It is hoped that this will eventually lead to the development of treatments that are less toxic and more effective than what surgery, chemotherapy, and radiation can currently offer.

III. METHODS

Cell lines and culture conditions. U2OS (osteosarcoma) (55), RD (ERMS) (56), Rh18 (fusion-negative ARMS) (56), Rh30 (t(2;13)-positive ARMS) (56), and Rh41 (t(2;13)-positive ARMS) (56) cells have been previously described in the literature. U2OS and RD cells were cultured in Dulbecco's Modified Eagle Medium (DMEM, Gibco) with L-glutamine and 4.5 g/L D-glucose containing 10% tetracycline-tested fetal bovine serum (FBS, Gibco), and Rh18, Rh30, and Rh41 cells were cultured in Roswell Park Memorial Institute 1640 Medium (RPMI, Gibco) with L-glutamine containing 10% FBS. The Tet-On 3G U2OS cell line was cultured in DMEM with L-glutamine and 4.5 g/L D-glucose, containing 10% FBS and 10 mg/mL blasticidin. The PAX3-FOXO1 clonal cell line as well as all clonal cell line candidates were cultured in DMEM with L-glutamine and 4.5 g/L D-glucose, containing 10% FBS, 10 mg/mL blasticidin, and 10 mg/mL puromycin. Expression of PAX3-FOXO1 was induced with 10 mg/ml doxycycline. All cells were maintained at 37°C with 5% CO_2. Unless otherwise indicated, all cells were washed with Dulbecco's Phosphate Buffered Saline (PBS, Gibco) and trypsinized with Trypsin-EDTA (0.25%) (Gibco).

Creation of PAX3-FOXO1 positive clonal cell line. PAX3-FOXO1 was chosen as the fusion protein of study because it is more prevalent than PAX7-FOXO1 in the ARMS patient population and has been associated with the worst clinical outcomes. The PAX3-FOXO1 sequence was obtained from the Barr Lab (National Cancer Institute) and amplified by PCR using the primers 5'-GATTATTATTAATCACCATGACCACGCTGGCC-3' and 3'-CACTAACCCATTAATTCAGCCTGACACCCAGC-5' with CloneAmp HiFi PCR

Premix (Clontech Laboratories). The reaction was run in the C1000 Touch Thermal Cycler (Bio-Rad Laboratories) under the following conditions: 95°C × 3 minutes, [98°C × 30 seconds, 65°C × 30 seconds, 72°C × 150 seconds] × 34 cycles, and 72°C × 5 minutes. After purification with the QIAquick PCR Purification Kit (Qiagen Corporation), the PCR products were cut with the restriction enzyme AseI (New England Biolabs (NEB)) under the manufacturer's suggested conditions (NEBuffer 3, incubated @ 37°C × 2 hours in the C1000 Touch Thermal Cycler). A pTRE-Tight vector (Clontech) was simultaneously cut with the restriction enzyme NdeI (NEB), again under the manufacturer's suggested conditions (NEBuffer 4, incubated @ 37°C × 2 hours). Both restriction-digest products were gel-purified using the QIAquick Gel Extraction Kit (Qiagen), modifying the manufacturer's instructions to omit the addition of isopropanol and the optional Buffer QG wash. The pTRE-Tight vector was then dephosphorylated with Antarctic Phosphatase (NEB) according to NEB protocol (incubated @ 37°C × 15 minutes). Following PCR purification of the vector with the QIAquick PCR Purification Kit, PAX3-FOXO1 was ligated into pTRE-Tight using T4 DNA Ligase (NEB) with the insert and vector in a 3.5:1 ratio.

The resulting plasmid was transformed into XL10-Gold Ultracompetent Cells (Agilent Technologies) per manufacturer specifications, and the cells were grown on soft agar with ampicillin overnight @ 37°C. Ten colonies were subsequently inoculated, and the plasmid was harvested from the bacteria using the QIAprep Spin Miniprep Kit (Qiagen). The ten plasmid samples were cut with the restriction enzyme HindIII (NEB) under the manufacturer's suggested conditions (NEBuffer 2, incubated @ 37°C × 2 hours), and the resulting products were run a 1% agarose ethidium bromide gel to verify that the PAX3-FOXO1 fusion gene was in the correct orientation within the vector. Of the ten samples

tested, two yielded the two bands of the expected size (2429 and 2948 bp). These two plasmids were sequenced at the Keck DNA Sequencing Facility (Yale School of Medicine) using the forward primer 5'-GATTATTATTAATCACCATGACCACGCTGGCC-3' for additional confirmation that the pTRE-Tight vector contained PAX3-FOXO1 in the correct orientation. This primer was directed against the PAX3-FOXO1 gene itself because of poor sequencing performance with primers directed against the pTRE-Tight vector. To check for point mutations within PAX3-FOXO1, the two plasmids were again sequenced, this time with four separate forward primers targeted to sequential segments of the fusion gene (5'-GACGCGGTCTGTGATCGAAACA-3', 5'-CTATACAGACAGCTTTGTGCCTC-3', 5'-CACCAGTTTGAATTCACCCAG-3', 5-CTTCTCCACCAGGAGAAGCTC-3') as well as one reverse primer (3'-GTACCTGCACAGGATCTTGGAGAC-5'). Based on these results, one of the two PAX3-FOXO1/pTRE-Tight plasmid candidates was selected for further use.

This plasmid was introduced into a U2OS cell line that stably expresses the Tet-On 3G transactivator (Clontech), received from the Jensen Lab (Yale School of Medicine). U2OS was selected as the host cell as it is a well-characterized cell line representative of mesenchymal tumors. Moreover, while multiple previous studies have chosen ERMS cells to serve as the host for inducible PAX3/7-FOXO1 systems based on the rationale that they better represent the overall milieu of ARMS cells, it was felt that U2OS cells provide a cleaner genetic background against which to study the effects of the fusion protein in isolation.

1×10^6 Tet-On 3G U2OS cells suspended in 100 μL Amaxa solution (Lonza Group) were nucleofected with 1 μg of the PAX3-FOXO1/pTRE-Tight construct and 50 ng of linear puromycin marker (Clontech). They were then plated on a 10-cm dish, with addition of

blasticidin and puromycin 24 hours later; the plates were then incubated until discrete colonies could be picked for growth in 96- and then 48-well plates. At this stage, each well was split into two wells of a 24-well plate. One well per clone was incubated with doxycycline for 24 hours before all cells were harvested for PAX3-FOXO1 expression screening by Western blot using anti-FOXO1 monoclonal antibody (Cell Signaling, C29H4). In total, over 90 candidates were screened.

Western blot protocol. All cells were lysed in 100-200 μL of RIPA buffer (50 mM HEPES, 250 mM NaCl, 5 mM EDTA, 1% NP40, H_2O to 50 mL) with protease inhibitor cocktail (Boehringer Mannheim Corporation). The samples were sonicated using the EpiShear Multi-Sample Sonicator/Chiller (Active Motif) for six cycles of 10 seconds on and 10 seconds off at 100% amplitude. The samples were then incubated at 95°C for 5 minutes and then centrifuged at room temperature for 1 minute. All samples were subsequently maintained at 4°C unless otherwise indicated.

To ensure equal loading of the protein, the sample concentrations were measured by Bradford assay (Bio-Rad) using the Synergy 2 microplate reader (BioTek Instruments Incorporated). The samples were diluted to a concentration of 1:10 in RIPA buffer, then prepared according to the manufacturer's Standard Procedure for Microtiter Plates and assessed in duplicate; five standards of 0.05 μg/μL, 0.1 μg/μL, 0.2 μg/μL, 0.4 μg/μL, and 0.5 μg/μL were used.

Each sample was prepared for loading with a target protein load of 25 μg, 1 mM of DTT (American Bioanalytical Incorporated), 8.25 μL of NuPAGE LDS Sample Buffer (4x) (Novex), and RIPA buffer to a total volume of 33 μL. Samples were run on 4-12% Bis-Tris

Protein Gels (Novex) in NuPAGE MOPS SDS running buffer (50 mM MOPS, 50 mM Tris base, 1 mM EDTA, 0.1% SDS to pH 7.7) at 100 mV. The proteins were transferred overnight at 33 mV at 4°C, using Immobilon-P transfer membrane (Millipore Corporation) and Mini Trans-Blot filter paper (Bio-Rad) with NuPAGE transfer buffer (25 mM bicine, 25 mM Bis-Tris, 1 mM EDTA, 20% methanol to pH 7.2) in the Mini Trans-Blot Electrophoretic Transfer Cell (Bio-Rad).

Following transfer, membranes were incubated in 5% milk in TBST (50 mM Tris-Cl, 150 mM NaCl to pH 7.6) for 1 hour, in primary antibody (anti-FOXO1 monoclonal antibody (Cell Signaling, C29H4) or anti-SMC1 monoclonal antibody (Abcam, ab21583)) in TBST for 1 hour, and in secondary antibody (anti-rabbit HRP-linked antibody (Cell Signaling, 7074)) in TBST for 1 hour. All incubations were carried out at room temperature, and membranes were washed four times for 10 minutes each between incubation steps. Membranes probed with a second primary antibody were first stripped with Restore PLUS Western Blot Stripping Buffer (Thermo Fisher Scientific) for 5 minutes at room temperature before the above protocol, starting with incubation in 5% milk, was repeated. All blots were developed using Amersham ECL Prime Western Blotting Detection Reagent (GE Healthcare Life Sciences), and analyzed using the ChemiDoc MP Imaging System and Image Lab software (Bio-Rad) per the manufacturers' protocols.

Validation of PAX3-FOXO1-positive clonal cell line as ARMS mimic. TaqMan (Thermo Fisher) data were obtained for Tet-On 3G U2OS, RD, Rh18, Rh30, Rh41, and the inducible PAX3-FOXO1 clonal cell lines to verify that the downstream genetic effects of PAX3-FOXO1 expression in the clone mirror those seen in fusion-positive ARMS cells. Three genes—DAPK (23, 31), FGFR4 (6, 14, 29, 31), and MyoD (6, 23, 25)—were selected as

proxies for global gene expression changes based on data previously reported in the literature and the proteins' native functions. Of note, GREM1 (23, 28, 29) was also initially selected as a proxy gene, but C_T values consistently failed to be read and the TaqMan probe was still under quality control investigation by the manufacturer at the time of writing.

RNA was obtained from the five control cell lines as well as uninduced and doxycycline-induced PAX3-FOXO1 clonal cells with the RNeasy Mini Kit (Qiagen Corporation). One pellet of approximately 10×10^6 cells was harvested per cell line, and suspended in 600 μL of Buffer RLT per manufacturer protocol. The optional DNase digestion and RNeasy spin column drying steps were included. Following RNA isolation, the purity of the samples were confirmed by NanoDrop (ThermoScientific) with a 260/280 nm ratio of ~2.0.

cDNA was generated from this RNA using the High Capacity cDNA Reverse Transcription Kit (Applied Biosystems) as per manufacturer protocol and using the C1000 Touch Thermal Cycler. For each 20 μL reaction, the upper limit of 2 μg of RNA was used. The resulting cDNA was subsequently used for a TaqMan assay (Applied Biosystems) with probes (Applied Biosystems) for DAPK (assay ID# Hs00234489_m1), FGFR4 (assay ID# Hs01106908_m1), MyoD (assay ID# Hs00159528_m1), and a reference (actin or 18S). Each PCR reaction contained the amount of cDNA resulting from 2 μg of corresponding RNA. All samples were run in triplicate per assay under the following conditions in the Mx3000P Real-Time PCR System (Agilent Technologies): 50°C × 2 minutes, 95°C × 10 minutes, and [98°C × 15 seconds, 60°C × 60 seconds] × 45 cycles. The data was processed using the accompanying MxPro QPCR software (Agilent Technologies).

The TaqMan assay was performed a total of three times. The first assay ("TaqMan

1") tested RD, Rh30, and Rh41 control cells as well as uninduced and doxycycline-induced (72 hours) PAX3-FOXO1 clonal cells, and primarily served to validate the use of the DAPK, FGFR4, and MyoD probes. The second assay ("TaqMan 2") tested RD, Rh18, Rh30, and Rh41 cells to further establish the relative levels of gene expression in the controls. Finally, the third assay ("TaqMan 3") tested Tet-On 3G U2OS, PAX3-FOXO1 clonal cells harvested after culture -/+ doxycycline induction for 72 hours, and PAX3-FOXO1 clonal cells harvested after culture -/+ induction for approximately two months.

The data for the RD, Rh18, Rh30, and Rh41 cell lines from TaqMan 1 and TaqMan 2 were used to verify that DAPK, FGFR4, and MyoD are significantly upregulated in fusion-positive ARMS cells and therefore valid proxies for confirming that the inducible PAX3-FOXO1 clonal cell line is a fusion-positive ARMS mimic. For each tested gene within an assay, the individual C_T values were normalized to the averaged C_T value for the reference gene (actin or 18S) for the corresponding cell line (individual C_T of tested gene – average C_T of reference gene) to generate three ΔC_T values per gene per cell line. These ΔC_T values were compared using the unpaired t-test (http://graphpad.com/quickcalcs/ttest1/) in order to demonstrate that the three genes are significantly upregulated in Rh30 and Rh41 cells as compared to RD and Rh18 cells. Mean ΔC_T values for each gene within each cell line were also calculated by averaging the C_T values from the triplicate samples and normalizing this value to the average C_T value of the reference gene of the corresponding cell line (average C_T of tested gene – average C_T of reference gene).

Following this, the data from TaqMan 1 and TaqMan 3 were used to assess the uninduced and doxycycline-induced PAX3-FOXO1 clonal cells in several ways. Mean ΔC_T values were first calculated for each gene per cell line condition as above. These values were

used to assess for statistically significant differential expression levels of DAPK, FGFR4, and MyoD in the clonal cell line compared to Tet-On 3G U2OS cells as well as to the four RMS control cell lines, again using the unpaired t-test. Additionally, the mean ΔC_T values were used to calculate $\Delta\Delta C_T$ values for each gene per doxycycline-induction time condition (72 hours or two months) by comparing the average ΔC_T for the control (uninduced) and experimental (induced) cell populations (ΔC_T uninduced – ΔC_T induced). The fold-change in target gene expression level was calculated as 2^(ΔΔCT).

Clonigenic survival assay of U2OS cells for future use in validating drug screen hits. A preliminary clonigenic survival assay of U2OS cells treated with etoposide was performed in order to verify the experimental conditions for future use in the validation of hits from the high-throughput chemical screen. U2OS cells were grown under the conditions described above to approximately 80% confluence on 25 10-cm plates, then incubated overnight in the presence of varying concentrations of etoposide (5 plates each for 0.1 μM, 1 μM, 5 μM, and 10 μM) or DMSO (hereafter labeled 0 μM). Following incubation, the cells for each drug concentration were trypsinized and combined in 2 mL of DMEM. Each of the five cell suspensions was counted in quadruplicate using the TC20 Automated Cell Counter (Bio-Rad Laboratories). These suspensions were then diluted to 9×10^5 cells/mL in 2 mL, then subsequently diluted to 9×10^3 cells/mL in 10 mL (1:10 dilution) and 4.5×10^3 cells/mL in 12 mL (1:2 dilution). The five 4.5×10^3 cells/mL stock solutions were serially diluted five times at a ratio of 1:3 to generate additional stock solutions of 1.5×10^3 cells/mL, 5×10^2 cells/mL, 1.665×10^2 cells/mL, 55.5 cells/mL, and 18.5 cells/mL per drug concentration. Of note, only the 4.5×10^3 cells/mL and 1.5×10^3 cells/mL stock solutions were created for the

10 μM-treated cells due to poor survival and low cell counts. 2 mL of each stock solution was plated in triplicate into 6-well plates, resulting in three 6-well plates per drug concentrations 0-5 μM and one 6-well plate for drug concentration 10 μM, and 13 plates for the assay overall.

The cells were incubated under standard conditions for 12 days before they were stained twice with crystal violet. Excess crystal violet solution was removed from the plates in a distilled water bath, and then allowed to air dry for approximately 24 hours. The stained colonies were manually counted.

The U2OS response to etoposide treatment was calculated as follows. The number of colonies in the triplicate wells per experimental condition were averaged, and then divided by the number of cells originally plated in order to calculate the fraction of cells that survived. For the control 0 μM condition only, all of these fractions were averaged in order to calculate the plating efficiency for the entire assay. Each calculated ratio of cells that survived was divided by this plating efficiency to generate a survival factor for each experimental condition (six original cell numbers per etoposide dose). The means of the survival factors for each dose of etoposide were then calculated to determine the overall U2OS dose-response to the drug.

IV. RESULTS

Tetracycline-inducible expression of PAX3-FOXO1 in U2OS clonal cell line. U2OS cells with conditional PAX3-FOXO1 expression were derived, as described in detail in the Methods. Although the intensity of the band corresponding to PAX3-FOXO1 (Figure 1) suggests that PAX3-FOXO1 levels are supra-physiological, the results of the TaqMan assays (Tables 1a vs. 2a vs. 3a vs. 4a), as further discussed below, indicate that downstream effects are on par with or even below what is observed in fusion-positive ARMS cells. The conditional induction of PAX3-FOXO1 expression provides an isogenic background with which to compare the effects of this fusion protein on gene expression and, in the future, the response to chemotherapeutic drug compounds.

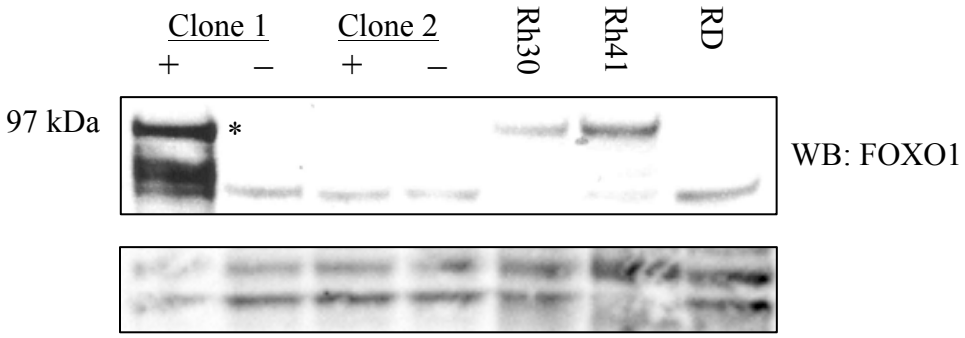

Figure 1. *Western blot showing tetracycline-inducible PAX3-FOXO1 expression in U2OS clonal cell line.* Whole-cell lysate samples were prepared and run as outlined in the Methods, and probed with anti-FOXO1 monoclonal antibody. +/- indicates doxycycline induction for 72 hours. Clone 1 positive for inducible expression of PAX3-FOXO1, indicated by * at expected size of ~97 kDa; Clone 2 negative for inducible expression. Rh30 and Rh41 are fusion-positive ARMS (positive control); RD is fusion-negative ERMS (negative control). Non-specific bands shown in place of SMC1 loading control.

The long-term stability of inducible expression of PAX3-FOXO1 was also tested. Unfortunately, despite robust levels of PAX3-FOXO1 for the first several weeks after the identification of the fusion-positive clone, expression begins to fall markedly thereafter (Figures 2a and 2b). However, the experiments for differential gene expression after transient transfection or in inducible systems of PAX3/7-FOXO1, as reported in the literature, were all conducted on a time scale of hours to several days after introduction of the fusion protein (23, 24, 28, 57); this is well within the window of stable expression for the cell line derived here. In addition, this loss of PAX3-FOXO1 expression over time incidentally allows for the investigation of the persistence of gene expression changes even after the fusion protein is essentially removed, as discussed below.

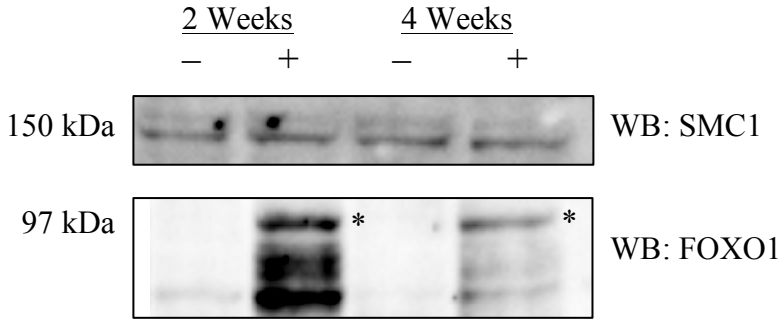

Figure 2a. *Western blot showing gradual loss of tetracycline-inducible PAX3-FOXO1 expression in U2OS clonal cell line.* Whole-cell lysate samples, from cells kept in culture for two and four weeks after initial validation of the clone, were prepared and run as outlined in the Methods, and probed with anti-FOXO1 monoclonal antibody followed by anti-SMC1 monoclonal antibody for loading control. -/+ indicates doxycycline induction for length of time indicated.

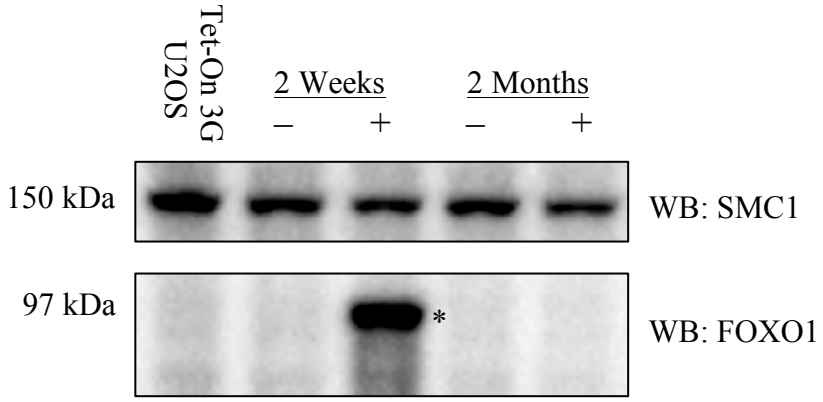

2b. *Western blot showing complete loss of tetracycline-inducible PAX3-FOXO1 expression in U2OS clonal cell line.* Whole-cell lysate samples, from cells kept in culture for two weeks and two months after initial validation of the clone, were prepared and run as outlined in the Methods, and probed with anti-FOXO1 monoclonal antibody followed by anti-SMC1 monoclonal antibody. -/+ indicates doxycycline induction for length of time indicated.

Validation of inducible PAX3-FOXO1 clonal cell line as fusion-positive ARMS mimic. The TaqMan assays to assess the validity of the inducible PAX3-FOXO1 U2OS clonal cell line, using DAPK, FGFR4, and MyoD as proxies for differential expression across the genome, yielded mixed but overall encouraging results. A comparison of C_T values from TaqMan 1 (Tables 1a and b) and TaqMan 2 (Tables 2a and b) for RD, Rh18, Rh30, and Rh41 cells confirmed that DAPK, FGFR4, and MyoD are in general upregulated in fusion-positive ARMS cells and therefore can be used to assess the inducible PAX3-FOXO1 clonal cell line. However, a number of caveats to these data must be noted. First, in TaqMan 1, the upregulation of DAPK in Rh41 cells relative to RD cells does not reach statistical significance (p-value < 0.05) (Table 1b), but in TaqMan 2 demonstrates a clear difference (Table 2b). Second, in TaqMan 1, the relative level of MyoD is higher than actin, as

represented by the negative ΔC_T value, in Rh41 cells (Table 1a); this seems intuitively incorrect, and such a phenomenon is not seen in TaqMan 2 although the reference gene in this case was 18S (Table 2a). Finally, the upregulation of MyoD in Rh30 cells relative to RD cells just reaches statistical significance in TaqMan 1 (Table 1b), but fails to do so in TaqMan 2 (Table 2b). Despite these inconsistencies, the data overall appeared to align with the literature and validate the decision to use DAPK, FGFR4, and MyoD, and so analysis of the inducible PAX3-FOXO1 cell line using these probes was performed.

	DAPK	FGFR4	MyoD
RD	6.017 (± 0.451)	13.330 (± 1.258)	2.213 (± 0.471)
Rh30	2.690 (± 0.509)	5.767 (± 1.022)	0.190 (± 0.410)
Rh41	5.677 (± 0.439)	8.260 (± 1.427)	-0.140 (± 0.490)

Table 1a. *ΔC_T values (± SD) from TaqMan 1 for DAPK, FGFR4, and MyoD expression in control cell lines.* C_T values from triplicate runs averaged, and then normalized to averaged actin C_T for corresponding cell line (average C_T of tested gene – average C_T of actin).

vs. RD	DAPK	FGFR4	MyoD
Rh30	0.0011	0.0010	0.0050
Rh41	0.4023	0.0114	0.0039

1b. *p-values for ΔC_T values from TaqMan 1 for DAPK, FGFR4, and MyoD upregulation in Rh30 and Rh41 cells compared to RD cells.* Individual C_T values were

normalized to the average C_T value for actin for the corresponding cell line (C_T of tested gene – average C_T of actin), and the resulting ΔC_T values for Rh30 and Rh41 were compared to those for RD using the unpaired t-test.

	DAPK	FGFR4	MyoD
RD	15.707 (± 0.012)	15.900 (± 0.066)	14.533 (± 1.246)
Rh18	17.380 (± 0.070)	16.237 (± 0.102)	25.347 (± 0.042)
Rh30	15.127 (± 0.079)	13.913 (± 0.091)	13.760 (± 0.047)
Rh41	9.023 (± 0.103)	8.503 (± 0.196)	6.427 (± 0.157)

Table 2a. *ΔC_T values (± SD) from TaqMan 2 for DAPK, FGFR4, and MyoD expression in control cell lines.* Calculations performed as in Table 1a, but normalized to 18S.

vs. RD	DAPK	FGFR4	MyoD
Rh30	0.0002	<0.0001	0.3432
Rh41	<0.0001	<0.0001	0.0004
vs. Rh18	DAPK	FGFR4	MyoD
Rh30	<0.0001	<0.0001	<0.0001
Rh41	<0.0001	<0.0001	<0.0001

2b. *p-values for ΔC_T values from TaqMan 2 for DAPK, FGFR4, and MyoD upregulation in Rh30 and Rh41 cells compared to RD and Rh18 cells.* Individual C_T values

were normalized to the average C_T value for 18S for the corresponding cell line (C_T of tested gene – average C_T of 18S), and the resulting ΔC_T values for Rh30 and Rh41 were compared to those for RD and Rh18 using the unpaired t-test.

In TaqMan 1, the expression of DAPK, FGFR4, and MyoD shows at least a two-fold increase after induction of PAX3-FOXO1 expression for 72 hours (Table 3b). However, the results are limited by the fact that no C_T values were read for two of the uninduced and one of the induced PAX3-FOXO1 samples for FGFR4, and therefore no standard deviation could be calculated for the ΔC_T or $\Delta\Delta C_T$ for this gene.

	DAPK	FGFR4	MyoD
PAX3-FOXO1 Clone (-)	17.877 (± 0.554)	25.200 (± N/A)	15.120 (± 0.593)
PAX3-FOXO1 Clone (+)	13.693 (± 0.372)	23.887 (± 2.729)	13.380 (± 0.405)

Table 3a. *ΔC_T values (± SD) from TaqMan 1 for DAPK, FGFR4, and MyoD expression in uninduced and induced PAX3-FOXO1 clonal cells.* Calculations performed as in Table 1a. -/+ indicates doxycycline induction for 72 hours.

	DAPK	FGFR4	MyoD
$\Delta\Delta C_T$	4.183 (± 0.667)	1.313 (± N/A)	1.740 (± 0.718)
Fold-change in expression	18.168	2.485	3.340

3b. *$\Delta\Delta C_T$ (± SD) and corresponding fold-changes in gene expression after induction of PAX3-FOXO1 expression, derived from TaqMan 1 data for DAPK, FGFR4, and MyoD.*

$\Delta\Delta C_T$ calculated as (ΔC_T uninduced – ΔC_T induced); ΔC_T values derived in 3a. Fold-change in expression calculated as $2^{(\Delta\Delta C_T)}$. Level of gene expression compared for PAX3-FOXO1 clonal cell line -/+ doxycycline induction for 72 hours.

The results of TaqMan 3 are both unexpected and encouraging. The most surprising finding was that DAPK, FGFR4, and MyoD have significantly lower levels of expression in both the uninduced and induced PAX3-FOXO1 clonal cell line conditions compared to the Tet-On 3G U2OS cells (Tables 4a and 4b). Although it was assumed that the uninduced PAX3-FOXO1 clonal cells would geerally share a genetic profile with the control Tet-On 3G U2OS cells, the expression of these three genes is lower in the clonal cell line compared to not only the Tet-On 3G U2OS cells but also RD, Rh18, Rh30, and Rh41 cells (Tables 2a, 4a, and 4c). This possibly suggests that the perturbation associated with PAX3-FOXO1 insertion may have disrupted normal levels of transcriptional activity. However, both the uninduced and induced PAX3-FOXO1 cells grow robustly and at approximately the same rate as the Tet-On 3G U2OS cells in culture, and with the same morphology, providing reassurance that whatever perturbation this may be is not disruptive to normal cellular function.

TaqMan 3 also shows that induction of the fusion protein is likely sufficient to induce ARMS-like genetic changes in the clonal cell line, and that sustained expression of PAX3-FOXO1 is necessary to maintain these changes. Both DAPK and MyoD are significantly upregulated in the cells induced with doxycycline for 72 hours; interestingly, however, FGFR4 sees a significant downregulation in the PAX3-FOXO1 induced state, which is inconsistent with the literature (6, 14, 29, 31) and also intuitively inconsistent with its known functions. The limited results of TaqMan 1, which imply that FGFR4 is upregulated in PAX3-FOXO1 expressing cells (Table 3b), better align with what would be expected of an

ARMS cell, but overall it is difficult to interpret the results for this gene without additional data from repeat experiments. On the other hand, none of the three genes tested demonstrate a significant difference in expression levels between the uninduced and induced cells that had been incubated for two months but lost PAX3-FOXO1 expression approximately one month prior to the assay (Table 4d).

	DAPK	FGFR4	MyoD
Tet-On 3G U2OS	15.827 (± 0.226)	9.567 (± 0.130)	18.387 (± 1.714)
PAX3-FOXO1 Clone (-), 72 hours	28.843 (± 0.180)	19.247 (± 0.026)	26.180 (± 0.110)
PAX3-FOXO1 Clone (+), 72 hours	24.740 (± 0.064)	19.777 (± 0.070)	25.057 (± 0.104)
PAX3-FOXO1 Clone (-), 2 months	28.843 (± 0.067)	19.247 (± 0.187)	26.180 (± 0.269)
PAX3-FOXO1 Clone (+), 2 months	27.710 (± 0.244)	19.660 (± 0.084)	26.320 (± 0.160)

Table 4a. *ΔC_T values (± SD) from TaqMan 3 for DAPK, FGFR4, and MyoD expression in Tet-On 3G U2OS, and uninduced and doxycycline-induced PAX3-FOXO1 clonal cells.* Calculations performed as in Table 1a, but normalized to 18S. -/+ indicates doxycycline induction for length of time specified, although with decline in PAX3-FOXO1 expression after ~1 month in the 2-month samples.

vs. Tet-On 3G U2OS	DAPK	FGFR4	MyoD
PAX3-FOXO1 Clone (-), 72 hours	<0.0001	<0.0001	0.0014

PAX3-FOXO1 Clone (+), 72 hours	<0.0001	<0.0001	0.0025
PAX3-FOXO1 Clone (-), 2 months	<0.0001	<0.0001	0.0016
PAX3-FOXO1 Clone (+), 2 months	<0.0001	<0.0001	0.0013

4b. *p-values for ΔC_T values from TaqMan 3 for DAPK, FGFR4, and MyoD levels in uninduced and doxycycline-induced PAX3-FOXO1 clonal cells, compared to Tet-On 3G U2OS cells.* Individual C_T values were normalized to the average C_T value for 18S for the corresponding cell line (C_T of tested gene – average C_T of 18S), and the resulting ΔC_T values for the inducible PAX3-FOXO1 cells under four experimental conditions were compared to those for Tet-On 3G U2OS using the unpaired t-test. -/+ indicates doxycycline induction for length of time specified, although with decline in PAX3-FOXO1 expression after ~1 month in the 2-month samples.

vs. RD	DAPK	FGFR4	MyoD
PAX3-FOXO1 Clone (-), 72 hours	<0.0001	<0.0001	<0.0001
PAX3-FOXO1 Clone (+), 72 hours	<0.0001	<0.0001	<0.0001
PAX3-FOXO1 Clone (-), 2 months	<0.0001	<0.0001	<0.0001
PAX3-FOXO1 Clone (+), 2 months	<0.0001	<0.0001	<0.0001
vs. Rh18	DAPK	FGFR4	MyoD
PAX3-FOXO1 Clone (-), 72 hours	<0.0001	<0.0001	0.0003
PAX3-FOXO1 Clone (+), 72 hours	<0.0001	<0.0001	0.0111
PAX3-FOXO1 Clone (-), 2 months	<0.0001	<0.0001	0.0157
PAX3-FOXO1 Clone (+), 2 months	<0.0001	<0.0001	0.0005

vs. Rh30	DAPK	FGFR4	MyoD
PAX3-FOXO1 Clone (-), 72 hours	<0.0001	<0.0001	<0.0001
PAX3-FOXO1 Clone (+), 72 hours	<0.0001	<0.0001	<0.0001
PAX3-FOXO1 Clone (-), 2 months	<0.0001	<0.0001	<0.0001
PAX3-FOXO1 Clone (+), 2 months	<0.0001	<0.0001	<0.0001
vs. Rh41	DAPK	FGFR4	MyoD
PAX3-FOXO1 Clone (-), 72 hours	<0.0001	<0.0001	<0.0001
PAX3-FOXO1 Clone (+), 72 hours	<0.0001	<0.0001	<0.0001
PAX3-FOXO1 Clone (-), 2 months	<0.0001	<0.0001	<0.0001
PAX3-FOXO1 Clone (+), 2 months	<0.0001	<0.0001	<0.0001

4c. *p-values for ΔC_T values from TaqMans 2 and 3 for DAPK, FGFR4, and MyoD levels in uninduced and doxycycline-induced PAX3-FOXO1 clonal cells, compared to RD, Rh18, Rh30, and Rh41 cells.* Individual C_T values were normalized to the average C_T value for 18S for the corresponding cell line (C_T of tested gene – average C_T of 18S), and the resulting ΔC_T values for the inducible PAX3-FOXO1 cells under the four experimental conditions were compared to those for the established RMS cell lines using the unpaired t-test. -/+ indicates doxycycline induction for length of time specified, although with decline in PAX3-FOXO1 expression after ~1 month in the 2-month samples.

	DAPK	FGFR4	MyoD
$\Delta\Delta C_T$, 72 hours	4.103 (± 0.191)	-0.530 (± 0.075)	1.123 (± 0.151)
Fold-change in expression, 72 hours	17.188	0.692	2.178

$\Delta\Delta C_T$, 2 months	0.033 (± 0.253)	0.197 (± 0.205)	0.340 (± 0.313)
Fold-change in expression, 2 months	1.023	0.873	0.790

4d. *$\Delta\Delta C_T$ (± SD) and corresponding fold-changes in gene expression after induction of PAX3-FOXO1 expression, derived from TaqMan 3 for DAPK, FGFR4, and MyoD.* Calculations performed as in Table 3b, but normalized to 18S; ΔC_T values derived in 4a. Levels of gene expression compared for PAX3-FOXO1 U2OS clonal cell line -/+ doxycycline induction for length of time specified, in PAX3-FOXO1 expression after ~1 month in the 2-month samples.

Clonigenic survival assay. U2OS cells demonstrate a dose-dependent response to overnight treatment with etoposide (Table 5 and Figure 3), with the greatest incremental effect noted between the 0 μM and 0.1 μM conditions. In addition to the poor cellular survival for the 10 μM condition at the outset of the experiment as noted in the Methods, the data faces two limitations. First, the cells were too confluent in the wells originally plated with 9×10^3 cells for the 0 μM and 0.1 μM treatment conditions and were therefore not included in the final calculations. Second, there were no surviving colonies in the wells originally plated with 111 cells for the 1 μM and 5 μM treatment conditions, nor in the wells originally plated with 37 cells for the 0.1 μM, 1 μM, and 5 μM treatment conditions; these were also omitted from the final calculations rather than being factored in as an individual survival factor of 0, as it seemed much more likely that the killing was non-specific rather than 100% effective at these drug concentrations. Yet even these limiting factors are consistent with a dose-dependent response to etoposide, and thus omission of the over-confluent and empty wells

diminishes the slope of the survival curve shown.

Etoposide Dose (μM)	0	0.1	1	5	10
Mean Survival Factor	1.000 (± 0.279)	0.374 (± 0.176)	0.190 (± 0.051)	0.157 (± 0.080)	0.113 (± 0.042)

Table 5. *Mean survival factors (± SD) of U2OS cells following overnight etoposide treatment at five different doses and 12 days of growth.* Mean survival factor was calculated by averaging the individual ratios of surviving to plated cells for each etoposide concentration, divided by the plating efficiency for the assay overall (the mean of the individual ratios for the 0 μM condition).

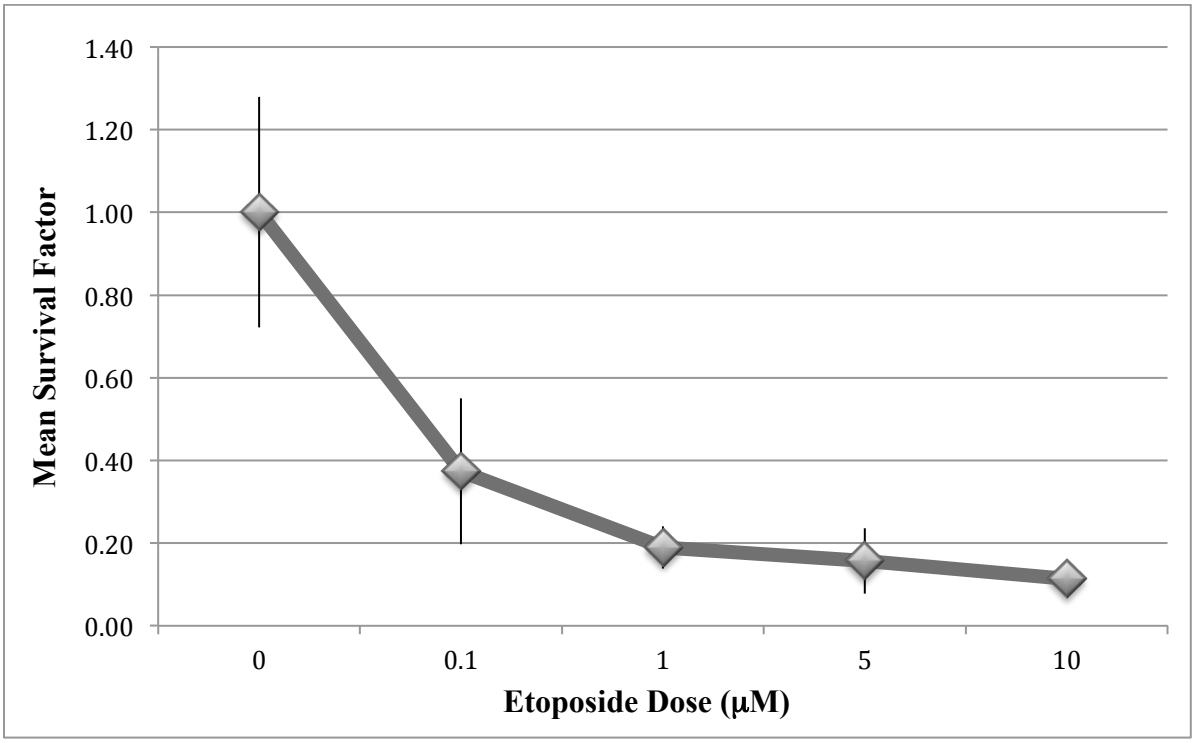

Figure 3. *Survival curve of U2OS cells following overnight etoposide treatment at five different doses and 12 days of growth.* See Table 5 for mean survival factor calculations and values. SDs of mean survival factors denoted by error bars.

V. DISCUSSION

An inducible PAX3-FOXO1 clonal cell line was created in U2OS cells using the Tet-On 3G and pTRE-Tight systems, and their validity as genetic mimics of fusion-positive ARMS cells was tested via cDNA analysis. Overall, the results of the TaqMan assays suggest that a 72-hour doxycycline induction of PAX3-FOXO1 expression in the cell line created here is sufficient to trigger the global changes in gene expression seen in fusion-positive ARMS cells, as represented by the upregulation in DAPK and MyoD, and possibly FGFR4. The differences in ΔC_T values between the uninduced and doxycycline-induced states reach statistical significance for DAPK and MyoD in both TaqMan assays performed, with a statistically significant greater than 17-fold increase for DAPK and greater than two-fold increase for MyoD between the uninduced to the induced states. The results for FGFR4 show likely upregulation in one TaqMan assay and downregulation in the other, and require further follow-up. GREM1 will also most likely be re-added in the future to provide additional support for the validity of using this clonal cell line for drug screens.

As mentioned above, the Western blots of the doxycycline-induced PAX3-FOXO1 whole cell lysates seem to suggest that the expression levels of the fusion protein are above physiological levels. However, a comparison of ΔC_T values for the inducible cell line and the Tet-On 3G U2OS, RD, Rh18, Rh30, and Rh41 cells indicates that the levels of DAPK, FGFR4, and MyoD are below physiological levels even in the doxycycline-induced state, providing reassurance that this system does not overestimate the effect of the fusion protein in the endogenous setting. In fact, the fact that the expression levels are lower than for the fusion-negative controls (Tet-On 3G U2OS, RD, and Rh18) potentially raises the concern that the potency of the tested drugs will be underestimated. It is difficult to predict this,

however, as the literature tends to agree on which genes are upregulated in fusion-positive ARMS and engineered cells but not on the actual fold-change in expression of these genes. Therefore, it will be necessary to work up the hits from the future drug screen in the inducible PAX3-FOXO1 clonal cell line as well as in fusion-positive and -negative ARMS cells.

The TaqMan assays also show that sustained expression of the fusion protein is necessary to maintain these transcriptional changes, as the levels of these three genes are not significantly different between the uninduced and induced states in the cells that lost PAX3-FOXO1 expression after continuous culture for two months. Therefore, the utility of these inducible cells in furthering the study of fusion-positive ARMS lies in the targeting of synthetically lethal relationships that evolve early in the course of PAX3-FOXO1 expression. Again, previous studies that used inducible systems also restricted their experiments to a similar time course, allowing for comparability of results, but it should be noted that constitutively expressing systems have revealed a greater number of upregulated genes than their inducible counterparts (23). The number of hits from any future drug screen may thus be limited by the relatively fewer synthetically lethal relationships at play.

From here, the uninduced and doxycycline-induced PAX3-FOXO1 clonal cells will be tested against each other in a high-throughput chemical screen that primarily focuses on inhibitors of DNA damage repair that are already in clinical use. Since the two cell populations will differ only in their expression of PAX3-FOXO1, any inhibitor that preferentially causes cell death in the induced cells can be assumed to target a DNA repair mechanism that has become synthetically lethal as a direct result of the fusion protein and not any number of the other genetic changes that have likely occurred in ARMS cells. These

inhibitors will be selected for confirmatory screens; the trial clonigenic assay of U2OS cells treated with etoposide provides a standard against which the experimental conditions for further workup of hits can be adjusted.

Incidentally, it is interesting to note that while DAPK, FGFR4, MyoD, and initially GREM1 were chosen as proxy genes based on a combination of the literature and endogenous function, only FGFR4 and MyoD, as discussed above, have been studied closely in the context of fusion-positive ARMS. The roles of DAPK and GREM1 have instead primarily been investigated in the broader context of mechanisms common to multiple cancers. While mechanistic studies of these genes are beyond the scope of this project, future research may reveal additional insight into the "transcriptional reprogramming" that PAX3/7-FOXO1 triggers.

What is known about DAPK is that it is active in apoptosis, autophagy, cell migration, and inflammation. It has typically been classified as a tumor suppressor that is downregulated secondary to increased methylation in many cancers (58). DAPK regulates cell death as well as cytoskeletal rearrangements, and lower levels of this protein have been correlated with increased metastasis (59). However, other studies have suggested that in certain contexts, DAPK may actually be pro-oncogenic (58), which would be more consistent with the RNA and cDNA data presented here and with the results of a number of previous studies (23, 28, 31). Additionally, FOXA1, a transcription factor in the same family as FOXO1, has been found to decrease the methylation status of DAPK in adenocarcinoma of the breast (60). Most intriguingly, DAPK has been found to be synthetically lethal to ER-negative breast, pancreatic, and ovarian cancer cells with p53 mutations (61). Although p53 mutations are typically not linked to ARMS and instead are more closely associated with

ERMS' genetic picture (62), there may be potential for DAPK to be synthetically lethal in ARMS secondary to mutations in or downregulation of other tumor suppressors.

Given its known endogenous functions, the role of GREM1 in the pathogenesis of ARMS is not difficult to imagine. It is an antagonist of BMP signaling, which in turn functions in embryonic and bone development (63); as discussed above, inhibition of terminal development and differentiation of muscle tissue is one of the key functions of PAX3/7-FOXO1. Independently of BMP signaling, GREM1 is a VEGF receptor-2 agonist that may therefore play roles in tumor-related angiogenesis (64) and enhance metastatic potential. The questions that surround DAPK's and GREM1's roles in fusion-positive ARMS serve as symbolic reminders that the mechanisms of the hits from chemical screens may not be well understood even when linked to a specific gene through follow-up or parallel siRNA screens.

There is clearly still much to be studied about RMS, and particularly fusion-positive ARMS, on multiple fronts. That ARMS disproportionately affects the pediatric population and carries a poor prognosis, while clinically discouraging, means that there are many potential life-years to be gained once this malignancy is better understood. This inducible PAX3-FOXO1 clonal cell line and the future high-throughput drug screen address just one of the challenges posed by this malignancy, but will hopefully open the door to not only identifying new targeted therapies but investigating the molecular and genetic pathways by which these therapies exert their specificity.

VI. REFERENCES

1. Howlader N, Noone AM, Krapcho M, Garshell J, Miller D, et al (eds). SEER Cancer Statistics Review (1975-2012), Section 32: Adolescent and Young Adult Cancer by Site Incidence, Survival, and Mortality [Internet]. Bethesda, MD: National Cancer Institute. 2015 Apr. Available from: http://seer.cancer.gov/csr/1975_2012/results_merged/sect_32_aya.pdf
2. Hettmer S, Li Z, Billin AN, Barr FG, Cornelison DD, et al. Rhabdomyosarcoma: current challenges and their implications for developing therapies. *Cold Spring Harb Perspect Med.* 2014 Nov;4(11):a025650.
3. Egas-Bejar D, and Huh WW. Rhabdomyosarcoma in adolescent and young adult patients: current perspectives. *Adolesc Health Med Ther.* 2014 Jun;5:115-125.
4. Breneman JC, Lyden E, Pappo AS, Link MP, Anderson JR, et al. Prognostic factors and clinical outcomes in children and adolescents with metastatic rhabdomyosarcoma--a report from the Intergroup Rhabdomyosarcoma Study IV. *J Clin Oncol.* 2003 Jan;21(1):78-84.
5. Arndt CA. Risk stratification of rhabdomyosarcoma: a moving target. *Am Soc Clin Oncol Educ Book.* 2013:415-419.
6. Davicioni E, Finckenstein FG, Shahbazian V, Buckley JD, Triche TJ, et al. Identification of a PAX-FKHR gene expression signature that defines molecular classes and determines the prognosis of alveolar rhabdomyosarcomas. *Cancer Res.* 2006 Jul;66(14):6936-6946.
7. De Giovanni C, Landuzzi L, Nicoletti G, Lollini PL, and Nanni P. Molecular and cellular biology of rhabdomyosarcoma. *Future Oncol.* 2009 Nov;5(9):1449-1475.
8. Parham DM, and Barr FG. Classification of rhabdomyosarcoma and its molecular basis. *Adv Anat Pathol.* 2013 Nov;20(6):387-397.
9. Skapek SX, Anderson J, Barr FG, Bridge JA, Gastier-Foster JM, et al. PAX-FOXO1 fusion status drives unfavorable outcome for children with rhabdomyosarcoma: a children's oncology group report. *Pediatr Blood Cancer.* 2013 Sep;60(9):1411-1417.
10. Sorensen PH, Lynch JC, Qualman SJ, Tirabosco R, Lim JF, et al. PAX3-FKHR and PAX7-FKHR gene fusions are prognostic indicators in alveolar rhabdomyosarcoma: a report from the children's oncology group. *J Clin Oncol.* 2002 Jun;20(11):2672-2679.
11. Missiaglia E, Williamson D, Chisholm J, Wirapati P, Pierron G, et al. PAX3/FOXO1 fusion gene status is the key prognostic molecular marker in rhabdomyosarcoma and significantly improves current risk stratification. *J Clin Oncol.* 2012 May;30(14):1670-1677.
12. Buckingham M, and Relaix F. PAX3 and PAX7 as upstream regulators of myogenesis. *Semin Cell Dev Biol.* 2015 Aug;44:115-125.
13. Matsuzaki H, Daitoku H, Hatta M, Tanaka K, and Fukamizu A. Insulin-induced phosphorylation of FKHR (Foxo1) targets to proteasomal degradation. *Proc Natl Acad Sci U S A.* 2003 Sep;100(20):11285-11290.
14. Charytonowicz E, Matushansky I, Domenech JD, Castillo-Martin M, Ladanyi M, et al. PAX7-FKHR fusion gene inhibits myogenic differentiation via NF-kappaB upregulation. *Clin Transl Oncol.* 2012 Mar;14(3):197-206.
15. Olanich ME, and Barr FG. A call to ARMS: targeting the PAX3-FOXO1 gene in

alveolar rhabdomyosarcoma. *Expert Opin Ther Targets.* 2013 May;17(5):607-623.
16. Xia SJ, and Barr FG. Analysis of the transforming and growth suppressive activities of the PAX3-FKHR oncoprotein. *Oncogene.* 2004 Sep;23(41):6864-6871.
17. Pandita A, Zielenska M, Thorner P, Bayani J, Godbout R, et al. Application of comparative genomic hybridization, spectral karyotyping, and microarray analysis in the identification of subtype-specific patterns of genomic changes in rhabdomyosarcoma. *Neoplasia.* 1999 Aug;1(3):262-275.
18. Shern JF, Chen L, Chmielecki J, Wei JS, Patidar R, et al. Comprehensive genomic analysis of rhabdomyosarcoma reveals a landscape of alterations affecting a common genetic axis in fusion-positive and fusion-negative tumors. *Cancer Discov.* 2014 Feb;4(2):216-231.
19. Weber-Hall S, Anderson J, McManus A, Abe S, Nojima T, et al. Gains, losses, and amplification of genomic material in rhabdomyosarcoma analyzed by comparative genomic hybridization. *Cancer Res.* 1996 Jul;56(14):3220-3224.
20. Goldstein M, Meller I, Issakov J, and Orr-Urtreger A. Novel genes implicated in embryonal, alveolar, and pleomorphic rhabdomyosarcoma: a cytogenetic and molecular analysis of primary tumors. *Neoplasia.* 2006 May;8(5):332-343.
21. Nishimura R, Takita J, Sato-Otsubo A, Kato M, Koh K, et al. Characterization of genetic lesions in rhabdomyosarcoma using a high-density single nucleotide polymorphism array. *Cancer Sci.* 2013 Jul;104(7):856-864.
22. van Gaal JC, Flucke UE, Roeffen MH, de Bont ES, Sleijfer S, et al. Anaplastic lymphoma kinase aberrations in rhabdomyosarcoma: clinical and prognostic implications. *J Clin Oncol.* 2012 Jan;30(3):308-315.
23. Ahn EH, Mercado GE, Lae M, and Ladanyi M. Identification of target genes of PAX3-FOXO1 in alveolar rhabdomyosarcoma. *Oncol Rep.* 2013 Aug;30(2):968-978.
24. Begum S, Emami N, Cheung A, Wilkins O, Der S, et al. Cell-type-specific regulation of distinct sets of gene targets by Pax3 and Pax3/FKHR. *Oncogene.* 2005 Mar;24(11):1860-1872.
25. Khan J, Bittner ML, Saal LH, Teichmann U, Azorsa DO, et al. cDNA microarrays detect activation of a myogenic transcription program by the PAX3-FKHR fusion oncogene. *Proc Natl Acad Sci U S A.* 1999 Nov;96(23):13264-13269.
26. Lae M, Ahn EH, Mercado GE, Chuai S, Edgar M, et al. Global gene expression profiling of PAX-FKHR fusion-positive alveolar and PAX-FKHR fusion-negative embryonal rhabdomyosarcomas. *J Pathol.* 2007 Jun;212(2):143-151.
27. Liu L, Wang YD, Wu J, Cui J, and Chen T. Carnitine palmitoyltransferase 1A (CPT1A): a transcriptional target of PAX3-FKHR and mediates PAX3-FKHR-dependent motility in alveolar rhabdomyosarcoma cells. *BMC Cancer.* 2012 Apr;12:154.
28. Mercado GE, Xia SJ, Zhang C, Ahn EH, Gustafson DM, et al. Identification of PAX3-FKHR-regulated genes differentially expressed between alveolar and embryonal rhabdomyosarcoma: focus on MYCN as a biologically relevant target. *Genes Chromosomes Cancer.* 2008 Jun;47(6):510-520.
29. Rapa E, Hill SK, Morten KJ, Potter M, and Mitchell C. The over-expression of cell migratory genes in alveolar rhabdomyosarcoma could contribute to metastatic spread. *Clin Exp Metastasis.* 2012 Jun;29(5):419-429.
30. Sun W, Chatterjee B, Wang Y, Stevenson HS, Edelman DC, et al. Distinct methylation profiles characterize fusion-positive and fusion-negative rhabdomyosarcoma. *Mod*

Pathol. 2015 Sep;28(9):1214-1224.
31. Wachtel M, Dettling M, Koscielniak E, Stegmaier S, Treuner J, et al. Gene expression signatures identify rhabdomyosarcoma subtypes and detect a novel t(2;2)(q35;p23) translocation fusing PAX3 to NCOA1. *Cancer Res.* 2004 Aug;64(16):5539-5545.
32. Carey KA, Segal D, Klein R, Sanigorski A, Walder K, et al. Identification of novel genes expressed during rhabdomyosarcoma differentiation using cDNA microarrays. *Pathol Int.* 2006 May;56(5):246-255.
33. Linardic CM, Naini S, Herndon JE, 2nd, Kesserwan C, Qualman SJ, et al. The PAX3-FKHR fusion gene of rhabdomyosarcoma cooperates with loss of p16INK4A to promote bypass of cellular senescence. *Cancer Res.* 2007 Jul;67(14):6691-6699.
34. Lagutina I, Conway SJ, Sublett J, and Grosveld GC. Pax3-FKHR knock-in mice show developmental aberrations but do not develop tumors. *Mol Cell Biol.* 2002 Oct;22(20):7204-7216.
35. Ren YX, Finckenstein FG, Abdueva DA, Shahbazian V, Chung B, et al. Mouse mesenchymal stem cells expressing PAX-FKHR form alveolar rhabdomyosarcomas by cooperating with secondary mutations. *Cancer Res.* 2008 Aug;68(16):6587-6597.
36. Naini S, Etheridge KT, Adam SJ, Qualman SJ, Bentley RC, et al. Defining the cooperative genetic changes that temporally drive alveolar rhabdomyosarcoma. *Cancer Res.* 2008 Dec;68(23):9583-9588.
37. Hartwell LH, Szankasi P, Roberts CJ, Murray AW, and Friend SH. Integrating genetic approaches into the discovery of anticancer drugs. *Science.* 1997 Nov;278(5340):1064-1068.
38. Shaheen M, Allen C, Nickoloff JA, and Hromas R. Synthetic lethality: exploiting the addiction of cancer to DNA repair. *Blood.* 2011 Jun;117(23):6074-6082.
39. Torti D, and Trusolino L. Oncogene addiction as a foundational rationale for targeted anti-cancer therapy: promises and perils. *EMBO Mol Med.* 2011 Nov;3(11):623-636.
40. Luo J, Solimini NL, and Elledge SJ. Principles of cancer therapy: oncogene and non-oncogene addiction. *Cell.* 2009 Mar;136(5):823-837.
41. Iglehart JD, and Silver DP. Synthetic lethality--a new direction in cancer-drug development. *N Engl J Med.* 2009 Jul;361(2):189-191.
42. Nijman SM. Synthetic lethality: general principles, utility and detection using genetic screens in human cells. *FEBS Lett.* 2011 Jan;585(1):1-6.
43. Weidle UH, Maisel D, and Eick D. Synthetic lethality-based targets for discovery of new cancer therapeutics. *Cancer Genomics Proteomics.* 2011 Jul-Aug;8(4):159-171.
44. Kaelin WG, Jr. The concept of synthetic lethality in the context of anticancer therapy. *Nat Rev Cancer.* 2005 Sep;5(9):689-698.
45. Iorns E, Lord CJ, Turner N, and Ashworth A. Utilizing RNA interference to enhance cancer drug discovery. *Nat Rev Drug Discov.* 2007 Jul;6(7):556-568.
46. Molenaar JJ, Ebus ME, Geerts D, Koster J, Lamers F, et al. Inactivation of CDK2 is synthetically lethal to MYCN over-expressing cancer cells. *Proc Natl Acad Sci U S A.* 2009 Aug;106(31):12968-12973.
47. Goga A, Yang D, Tward AD, Morgan DO, and Bishop JM. Inhibition of CDK1 as a potential therapy for tumors over-expressing MYC. *Nat Med.* 2007 Jul;13(7):820-827.
48. den Hollander J, Rimpi S, Doherty JR, Rudelius M, Buck A, et al. Aurora kinases A and B are up-regulated by Myc and are essential for maintenance of the malignant state. *Blood.* 2010 Sep;116(9):1498-1505.

49. Yang D, Liu H, Goga A, Kim S, Yuneva M, et al. Therapeutic potential of a synthetic lethal interaction between the MYC proto-oncogene and inhibition of aurora-B kinase. *Proc Natl Acad Sci U S A.* 2010 Aug;107(31):13836-13841.
50. Rottmann S, Wang Y, Nasoff M, Deveraux QL, and Quon KC. A TRAIL receptor-dependent synthetic lethal relationship between MYC activation and GSK3beta/FBW7 loss of function. *Proc Natl Acad Sci U S A.* 2005 Oct;102(42):15195-15200.
51. Wang Y, Engels IH, Knee DA, Nasoff M, Deveraux QL, et al. Synthetic lethal targeting of MYC by activation of the DR5 death receptor pathway. *Cancer Cell.* 2004 May;5(5):501-512.
52. Fam HK, Walton C, Mitra SA, Chowdhury M, Osborne N, et al. TDP1 and PARP1 deficiency are cytotoxic to rhabdomyosarcoma cells. *Mol Cancer Res.* 2013 Oct;11(10):1179-1192.
53. Zeng FY, Cui J, Liu L, and Chen T. PAX3-FKHR sensitizes human alveolar rhabdomyosarcoma cells to camptothecin-mediated growth inhibition and apoptosis. *Cancer Lett.* 2009 Nov;284(2):157-164.
54. Brough R, Frankum JR, Costa-Cabral S, Lord CJ, and Ashworth A. Searching for synthetic lethality in cancer. *Curr Opin Genet Dev.* 2011 Feb;21(1):34-41.
55. Ponten J, and Saksela E. Two established in vitro cell lines from human mesenchymal tumours. *Int J Cancer.* 1967 Sep;2(5):434-447.
56. Hinson AR, Jones R, Crose LE, Belyea BC, Barr FG, et al. Human rhabdomyosarcoma cell lines for rhabdomyosarcoma research: utility and pitfalls. *Front Oncol.* 2013 Jul;3:183.
57. Ginsberg JP, Davis RJ, Bennicelli JL, Nauta LE, and Barr FG. Up-regulation of MET but not neural cell adhesion molecule expression by the PAX3-FKHR fusion protein in alveolar rhabdomyosarcoma. *Cancer Res.* 1998 Aug;58(16):3542-3546.
58. Huang Y, Chen L, Guo L, Hupp TR, and Lin Y. Evaluating DAPK as a therapeutic target. *Apoptosis.* 2014 Feb;19(2):371-386.
59. Chen HY, Lee YR, and Chen RH. The functions and regulations of DAPK in cancer metastasis. *Apoptosis.* 2014 Feb;19(2):364-370.
60. Zheng L, Qian B, Tian D, Tang T, Wan S, et al. FOXA1 positively regulates gene expression by changing gene methylation status in human breast cancer MCF-7 cells. *Int J Clin Exp Pathol.* 2015 Jan;8(1):96-106.
61. Zhao J, Zhao D, Poage GM, Mazumdar A, Zhang Y, et al. Death-associated protein kinase 1 promotes growth of p53-mutant cancers. *J Clin Invest.* 2015 Jul;125(7):2707-2720.
62. Seki M, Nishimura R, Yoshida K, Shimamura T, Shiraishi Y, et al. Integrated genetic and epigenetic analysis defines novel molecular subgroups in rhabdomyosarcoma. *Nat Commun.* 2015 Jul;6:7557.
63. Brazil DP, Church RH, Surae S, Godson C, and Martin F. BMP signalling: agony and antagony in the family. *Trends Cell Biol.* 2015 May;25(5):249-264.
64. Mitola S, Ravelli C, Moroni E, Salvi V, Leali D, et al. Gremlin is a novel agonist of the major proangiogenic receptor VEGFR2. *Blood.* 2010 Nov;116(18):3677-3680.
65. Khan J, Simon R, Bittner M, Chen Y, Leighton SB, et al. Gene expression profiling of alveolar rhabdomyosarcoma with cDNA microarrays. *Cancer Res.* 1998 Nov;58(22):5009-5013.
66. De Pitta C, Tombolan L, Albiero G, Sartori F, Romualdi C, et al. Gene expression

profiling identifies potential relevant genes in alveolar rhabdomyosarcoma pathogenesis and discriminates PAX3-FKHR positive and negative tumors. *Int J Cancer.* 2006 Jun;118(11):2772-2781.
67. Armeanu-Ebinger S, Bonin M, Habig K, Poremba C, Koscielniak E, et al. Differential expression of invasion promoting genes in childhood rhabdomyosarcoma. *Int J Oncol.* 2011 Apr;38(4):993-1000.
68. Hu K, Lee C, Qiu D, Fotovati A, Davies A, et al. Small interfering RNA library screen of human kinases and phosphatases identifies polo-like kinase 1 as a promising new target for the treatment of pediatric rhabdomyosarcomas. *Mol Cancer Ther.* 2009 Nov;8(11):3024-3035.
69. Sullivan LM, Atkins KA, LeGallo RD. PAX immunoreactivity identifies alveolar rhabdomyosarcoma. *Am J Surg Pathol.* 2009 May;33(5):775-780.
70. Bennani-Baiti IM, Machado I, Llombart-Bosch A, Kovar H. Lysine-specific demethylase 1 (LSD1/KDM1A/AOF2/BHC110) is expressed and is an epigenetic drug target in chondrosarcoma, Ewing's sarcoma, osteosarcoma, and rhabdomyosarcoma. *Hum Pathol.* 2012 Aug;43(8):1300-1307.